Journal of Electronic Testing (2024) 40:87–99
https://doi.org/10.1007/s10836-024-06103-z

Reactant and Waste Minimization during Sample Preparation on Micro-Electrode-Dot-Array Digital Microfluidic Biochips using Splitting Trees

Chen Dong[1,3] · **Xiao Chen**[1] · **Zhenyi Chen**[2]

Received: 8 September 2023 / Accepted: 18 January 2024 / Published online: 7 March 2024

Abstract
Biological assays around "lab-on-a-chip (LoC)" are required in multiple concentration (or dilution) factors, satisfying specific sample concentrations. Unfortunately, most of them suffer from non-locality and are non-protectable, requiring a large footprint and high purchase cost. A digital geometric technique can generate arbitrary gradient profiles for digital microfluidic biochips (DMFBs). A next- generation DMFB has been proposed based on the microelectrode-dot-array (MEDA) architectures are shown to produce and disperse droplets by channel dispensing and lamination mixing. Prior work in this area must address the problem of reactant and waste minimization and concurrent sample preparation for multiple target concentrations. This paper proposes the first splitting-droplet sharing algorithm for reactant and waste minimization of multiple target concentrations on MEDAs. The proposed algorithm not only minimizes the consumption of reagents but also reduces the number of waste droplets by preparing the target concentrations concurrently. Experimental results on a sequence of exponential gradients are presented in support of the proposed method and demonstrate its effectiveness and efficiency. Compared to prior work, the proposed algorithm can achieve up to a 24.8% reduction in sample usage and reach an average of 50% reduction in waste droplets.

Keywords Microelectrode-dot-array (MEDA) · Biochip · Mixing tree · Dilution · Sample preparation · Reactant minimization

1 Introduction

To meet the challenges of healthcare costs for cardiovascular diseases, cancer, diabetes, global HIV crisis, and so on, a new field of interdisciplinary research centered around "lab-on-a-chip (LoC)" is emerging, which implements one or more biochemical laboratory protocols on a single chip [4, 27]. The worldwide market for in vitro diagnostics in 2007 was estimated at $38 billion, and 1.5 billion diagnostic tests per year worldwide have been predicted for malaria alone [27]. Sample preparation is an indispensable step in almost all biochemical protocols for mixing two or more biochemical reagents in a given volumetric ratio [2], called target concentration factor (CF), where 95% of cost mostly depends on the consumption of valuable reactants [11]. Dilution gradients can regulate the degree of diffusion [14] and play an essential role in practice, e.g., in digital polymerase chain reaction (digital PCR, dPCR) [35], where template, enzyme inactivation, and primer quality affect false-negative amplification results [23, 25, 29]. Another example of an accurate assay is the enzymatic glucose assay (Trinder's reaction) [13, 26], which requires several reagents with different concentration levels.

Responsible Editor: K. Chakrabarty

Xiao Chen and Zhenyi Chen are authors contributed equally to this work.

✉ Chen Dong
dongchen@fzu.edu.cn

Xiao Chen
chenxiao20220118@163.com

Zhenyi Chen
zhenyichen@usf.edu

[1] College of Computer and Data Science, Fuzhou University, Xueyuan Rd., Fuzhou 350116, Fujian, China

[2] Department of Computer Science and Engineering, University of South Florida, Tampa Bay, Tampa 33620, Florida, USA

[3] Fujian Key Laboratory of Network Computing and Intelligent Information Processing, Fuzhou University, Xueyuan Rd., Fuzhou 350116, Fujian, China

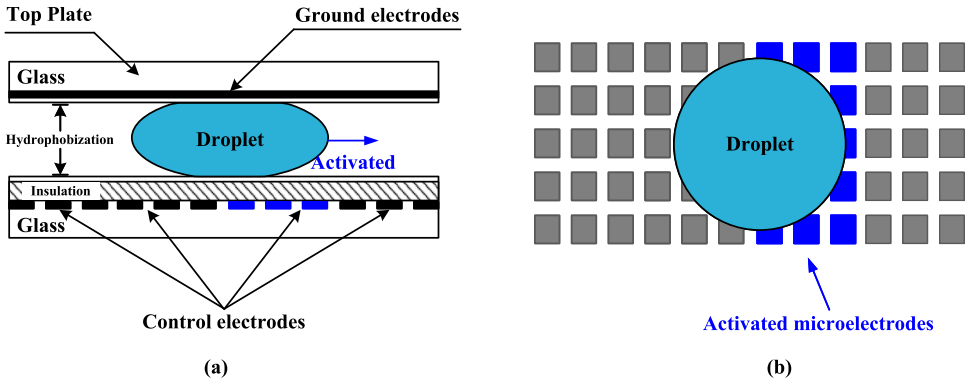

Fig. 1 A droplet undergoing transport on a MEDA biochip: **a** Side view and **b** Top view

Designs of such gradient generators on digital microfluidic biochips (DMFBs) were reported in [5, 22, 30, 32, 33], which have the advantages of high precision, small consumption, and high flexibility in experimental places [4, 6, 8]. Prototypes of MEDA-based biochips have been fabricated using the TSMC 0.35 μm CMOS technology [24]. Moreover, a cloud-based open-source electrowetting-on-dielectric (EWOD) cyber-manufacturing ecosystem [7, 8] has been applied during the sample preparation, where DMFBs only utilize the (1:1) mixing model [34]. As shown in Fig. 1, next-generation DMFBs, MEDAs allow microelectrodes to be dynamically grouped to form a micro-component that can perform novel microfluidic operations on the chip [18, 34]. One of the operations is channel dispensing, which controls the sizes of the two resultant droplets on MEDA biochips. Fig. 2 illustrates the three steps in which the droplet completes splitting on the chip.

MEDAs also provide another novel merging operation named lamination mixing. Two different sizes of droplets, e.g., a 1X and a 3X volume droplet, can be combined into a 4X volume droplet (Fig. 3(a-b)). A general mixing model (s_1: s_2:...: s_n) has been proposed in [19], where n is the number of droplets that are mixed, and s_i represents the respective volume size of droplet i.

It is a potentially important application of MEDA biochips to mix with buffer droplets until the target concentration via a series of channel dispensing and lamination mixing on MEDAs [24]. Although the generic multiple-reactant algorithm was proposed in [16, 20], which exploits such novel operations, However, existing MEDA-based dilution algorithms [15, 17] do not consider the arithmetic properties embedded in the gradient pattern while optimizing the cost. In this paper, we utilize the underlying combinatorial properties of exponential concentration gradients to produce the desired target ratios lying on the gradient profile by extending dispensing and mixing on MEDAs. The splitting-droplet sharing algorithm on MEDAs is proposed, which decomposes the inputs to minimize the required sample droplets and waste production. The proposed algorithm consists of three stages:

- The ratio decomposition stage
- The splitting graph construction stage
- The waste droplet-sharing stage

The first stage determines the best decomposition of the splitting chart's input, and the second stage constructs the splitting graph representing the target CF. And the third is aiming at waste droplet recycling for the same target. Extensive simulation results are presented to compare the proposed methods with several state-of-the-art multi-target dilutions algorithms [2, 9, 10, 12]. Results show that, compared to prior methods, the proposed method can achieve up to 24.80%.

The remainder of this paper is organized as follows. Section 2 gives the formulation of the problem of on-chip sample preparation for dilutions of multi-target CF. Section 3 builds a splitting model for the issue of Section 2. Section 4 presents the proposed algorithm for multi-target CF and an example demonstration with single CF and multi-CF cases. Section 5 shows the simulation results, including several synthetic test dilution cases. Finally, conclusions and future works are drawn in Section 6.

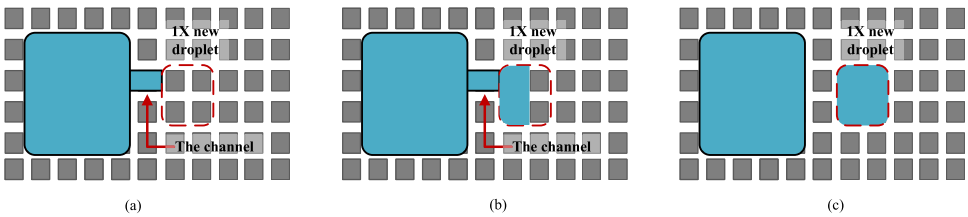

Fig. 2 Channel dispensing. **a** A 4X droplet forms a channel toward the new droplet. **b** A 1X droplet is derived from the channel. **c** The channel breaks in the middle, generating two resultant droplets, 1X and 3X volume

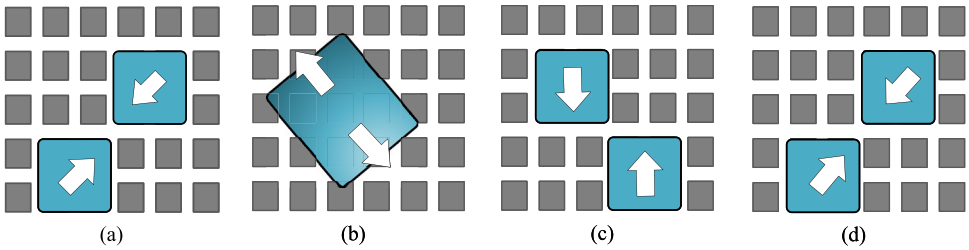

Fig. 3 Lamination mixing [19]. **a** Two droplets are merged. **b** The merged droplet is split in the direction that is orthogonal to the merged direction. **c** Two split droplets are transported to the start positions respectively. **d** The same operations are repeated until the droplet is mixed completely

2 Background

2.1 Sample Preparation on DMFBs

It is accomplished by a sequence of droplet-mix-split steps on a biochip, where many real-life applications require a sample with multiple concentration factors (CF) [24]. When the output droplet concentration is single, it is called single target sample preparation. When the output concentration is two or more, it is collectively called multi-target sample preparation.

2.1.1 Mixing Model on DMFBs

Mixing the k unit volume of one droplet with the t unit volume of another droplet produces a mixture of $(k+t)$ unit volume in a mix-and-split, called the $(k: t)$ mixing model.

When a droplet with $CF = c_1$ is mixed with another droplet with $CF = c_2$ and $c_2 < c_1$, dilution can be achieved for $c_3 = (c_1 + c_2)/2$, where c_3 meet $c_2 < c_3 < c_1$ after a mix-and-split operation. When the expected accuracy level is h, the predicted target CF is represented as a h-bit binary fraction (truncating it beyond h_{th} bits).

2.1.2 Dilution Using Mixing Tree on DMFBs

Mixing tree is proposed in BS [31] based on DMFBs, where the operations are executed level by level from the rightmost least significant bit (LSB) to the leftmost most significant bit (MSB) and are dependent on the bit string - "1" represents a raw reactant, while "0" indicates a buffer.

Figure 4 compares the execution processes of BS [31] during single target preparation. According to the mixing principle of $c_3 = (c_1 + c_2)/2$, the final product $\frac{317}{1024}$ is composed of a mixture of $\frac{512}{1024}$ and $\frac{112}{1024}$, $\frac{96}{1024}$ is composed of a mixture of $\frac{64}{1024}$ and $\frac{112}{1024}$, and $\frac{608}{1024}$ is composed of a mixture of $\frac{1024}{1024}$ and $\frac{192}{1024}$.

RSM [12], and REMIA [11] have adopted mixing trees and improved their defects in sample consumption. Fig. 5a shows a tree built in REMIA [11] proposed way.

- Two droplets with a concentration of $\frac{512}{1024}$ were generated by a mix-and-split operation with a sample concentration and a buffer concentration.
- The resulting droplets with a concentration of $\frac{512}{1024}$ mixed with buffer droplets and split.
- A droplet with a concentration of $\frac{256}{1024}$ and a sample has generated two target concentration droplets, namely $(\frac{256}{1024} + 1)/2 = 2\frac{608}{1024}$.

Therefore, when given target CF is $\frac{608}{1024}$, it was two operations, two buffers, and two waste to prepare two droplets with target CFs of $\frac{608}{1024}$, where the target ratio is {608}.

Similarly, two-target generation is shown in Fig. 5b. There were seven operations on a DMFB to prepare target concentrations of $\frac{608}{1024}$ and $\frac{96}{1024}$, using two reagents and five buffers throughout the process, resulting in three waste. Two concentrations of $\frac{96}{1024}$ and $\frac{608}{1024}$ were generated during the sixth and seventh operations, respectively.

2.2 Literatures and Motivations

Over the last decade, a lot of research work has been done on algorithm design for the automation of (1:1) mixing model on DMFBs, all of which focus on achieving

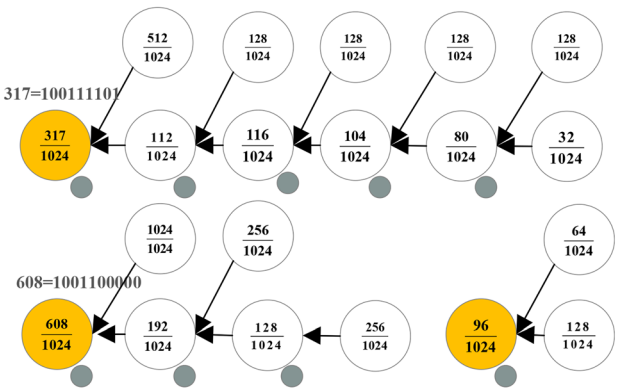

Fig. 4 Mixing trees for $\frac{608}{1024}$, $\frac{96}{1024}$ and $\frac{317}{1024}$

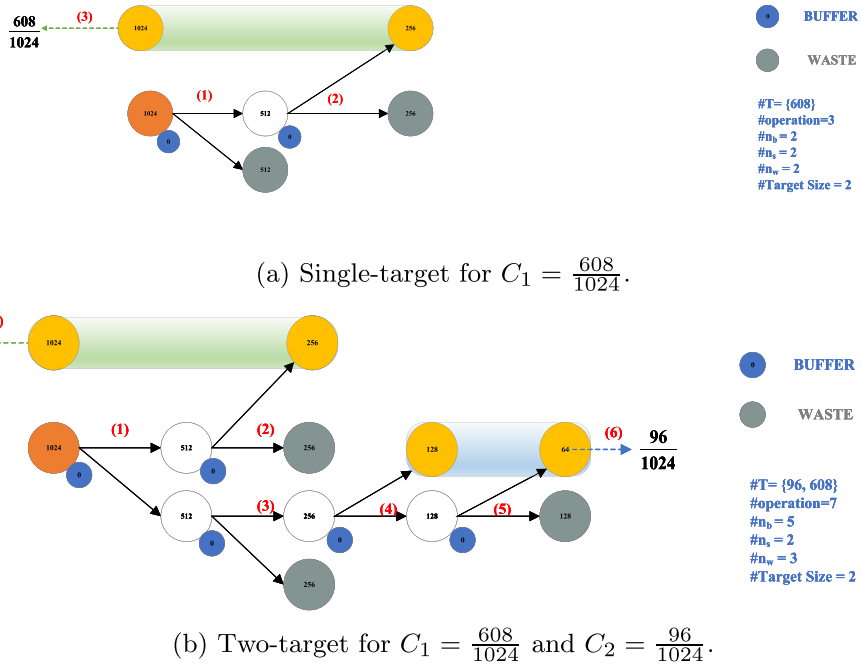

Fig. 5 REMIA [11] for different CFs

(a) Single-target for $C_1 = \frac{608}{1024}$.

(b) Two-target for $C_1 = \frac{608}{1024}$ and $C_2 = \frac{96}{1024}$.

sample/waste minimization [2, 10–12, 21, 28]. REactant-MInimization Algorithm [11] (REMIA) was proposed first to minimize reactant usage on DMFBs. Exponential Dilution Algorithm [2] (EDT) was reported for efficient generations of dilution gradients while reducing the cost of reactants (sample/buffer), based on (1:1) modeling on DMFBs. Dilution algorithms have been also proposed for MEDA biochips [15, 17]. The weighted sample-preparation method (WSPM) has been published as the first dilution approach for MEDA biochips to generate a dilution strategy [17]. Later, a more efficient dilution approach and a volume-oriented dilution approach, called FacDA and TVODA, respectively, were designed in [15], all shown in Table 1.

Motivation: The main objective in sample preparation is to minimize (1) the volume of the sample needed; (2) the number of generated waste droplets [24]. Existing algorithms have been proven effective while attempting to share the operations to reduce reactant cost and waste-production amount. However, it is challenging to achieve a gradient dilution using the minimum number of reagents with a minimum waste on a DMFB [1]. When the concentration limit of the sample source droplet is 1 (i.e., 100%), almost all DMFB algorithms have the problem of unavoidable waste droplet generation [2]. Motivated by an example described by EDT [2] on DMFBs, we present an algorithm for producing any given exponential dilution gradient with minimum wastage. In other words, total reagent consumption is minimized.

Table 1 Dilution algorithms

Dilution algorithm	Aims to reduce waste?	Aims to reduce reactant?	Produces multiple target-CFs?	Sizes of target set?
WSPM [17]	YES	YES	NO	1
DFM [15]	YES	YES	NO	1
FacDA [15]	YES	YES	NO	1
REMIA [11]	NO	YES	YES	1
EDT [2]	YES	YES	NO	1
Proposed	YES	YES	YES	$[1, 2^{10}]$

Table 2 Notations and Descriptions

Notations	Descriptions
h	Precision level of dilution.
C	A Set of exponential-gradient target CFs.
T	A Set of exponential-gradient target ratios.
n	Number of different target CF in C.
node	Output droplets with different concentrations.
Q	A Set of *node*.
TargetSize	Number of output droplets.
ST	Represents the process of generating target Q.
GST	A Set of minimum *ST*.
w	A set of wastage CF in *GST*.
K	Minimum wastage CF in *GST*.
RST	Ratio of *ST* new sources with concentration K.

2.3 Problem Formulation

Dilution can now be formally stated as follows. The prominent notation used in this paper is summarized in Table 2.

1. The *inputs* are as follows.
   (a) Required droplets' size *TargetSize*, where *TargetSize* is the r power of 2.
   $$TargetSize = 2^r$$
   (b) The precision level of concentration representation h.
   (c) A set of target CF C.
   $$C = \{C_1, C_2, \cdots, C_n\}$$
   where n is number of required different concentrations.
   (d) A Set of exponential gradient ratios for target ratios T.
   $$T = \{T_1, T_2, \cdots, T_n\}$$
   Element $T_i \in T$ specifies the portions of each CF C_i as given by the following equation:
   $$C_i = \frac{T_i}{2^h} \tag{1}$$
   where $i = 1, 2, \cdots, n$, and h is positive integer.
2. The *outputs* are as follows.
   (a) A set of wastage CF w.
   $$w = \{w_1, w_2, \cdots, w_x\}$$
   where x is number of different wastage CFs.
   (b) The number of sample n_s and waste n_w.
3. The objectives are as follows.
   (a) To determine a ratio algebraic expressions *RST* for T in size.
   (b) To build *ST* that can generate target CF.
   (c) The algorithm proposed improves waste minimization and sample saving.

3 Proposed Splitting Tree Model

3.1 Splitting Tree

A sample generation process for dilution is modeled using a tree structure named splitting tree (*ST*), and then droplets with concentration of source CF can be said to be discrete and dispersed into *TargetSize* droplets. The following definition gives notations for dilution droplet generation.

Definition 1 Splitting Rule (*SR*):

- The concentration of $node_{root}$ is source CF.
- There is only one droplet $node_{root}$ that begins to split, and the concentration of that droplet satisfies v_{right} <= source CF.
- The droplet undergoes splitting to produce two droplets of equal concentration and sequential order.
- Splitting does not produce waste droplets.

Definition 2 Splitting Tree (*ST*): According to *SR*, *ST* is a finite set with nodes n_{tree} ($n_{tree} > 0$).

- $ST \neq \emptyset$.
- Each splitting behavior obeys the *SR*.

$$h = \lceil log_2 TargetSize \rceil \tag{2}$$

$$unit\ size = 2^h \tag{3}$$

$$unit\ CF\ = v_{2^h-1} = v_{2^h-2} = \cdots = v_{2^{h-1}} = \frac{1}{2^h} \tag{4}$$

where *unit CF* is the concentration of layer h, and *unit size* is the maximum node number of this layer.

Definition 3 *node* pepresents the droplets with different output CFs v and number of droplets with different CF s.

$$node =< s, v > \tag{5}$$

$$drop = \begin{cases} true & v = c \\ false & otherwise \end{cases} \tag{6}$$

$$TargetSize = \sum s \tag{7}$$

When *drop* is true, it is represented that the output concentration v meets the standard within the error range, and then the splitting proceeds to the next sub-tree; otherwise, the *ST* generation steps will not continue. The number of *node* generated by *ST* ranges from 2^{h-1} to $2^h - 1$, where *drop* are true, and v are equal $\frac{1}{2^h}$.

Definition 4 n represents the set size of T, Q is set of droplets with $node_i$ generated by *ST*, and V represents the sum of droplet volumes used for sample preparation.

$$Q = \langle node_1, \cdots node_i, \cdots node_n \rangle \tag{8}$$

3.2 Proposed Algorithm

Algorithm 1 describes a single target preparation in which products target CF v and its quantity s. Eq. 4 is the relationship between concentrations of leaf nodes *unit CF* and tree height h, so h is obtained from input target CF (line 2), $drop = true$ indicating the completion of mix-and-split operations, where no node can be split in Q (line 4). According to Eq. 3, the i_{th} layer can generate up to N_{MAX} nodes (line 5) and s is quantity of Q (line 6). While $s \leq N_{MAX}$, the *node* in Q combines with a buffer for a mix-and-split operation, resulting in *ST* mix-and-split downwards (line 8-15). From the result queue Q, the queue head element *node* is dequeued (line 8), *node* is used as the parent node in the *ST* to generate (lines 12-13), which enters Q from the tail (line 14). The above process assumes that *drop* is true, indicating that it is the target CF, and the generation of *node* is ended (lines 9-11). When *TargetSize* is up to N_{MAX}, it indicates that no mix-and-split is performed (lines 16-17).

Algorithm 1 Splitting Tree Generation Algorithm

```
Require: T
Ensure: Q
1:  Q ⇐ CreatQueue(source CF)
2:  h ⇐ ⌈log2 1/target CF⌉
3:  i ⇐ −1
4:  while there exists an element node ∈ Q, i ≤ h do
5:      N_MAX ⇐ 2^i
6:      s ⇐ −1
7:      while s ≤ N_MAX do
8:          node ⇐ DelQueue(Q)
9:          if drop == true then
10:             continue
11:         end if
12:         node ⇐ Split(node)
13:         Update s
14:         AddQueue(Q, node)
15:     end while
16:     i ⇐ i + 1
17: end while
```

3.2.1 Example: Single-Target Preparation

ST construction is to produce Q where contains target CF drops. The root of an *ST* always has a concentration of 1. Since a mix-and-split operation produces two resultant droplets, the out-degree of a branch node is at most two. A branch node may have only one child, which implies only one resultant droplet is required for succeeding operations, and the other one is thus discarded as waste. According to the above facts, an *ST* is a binary tree but is not necessarily a full one. When $drop$ = true, it indicates that v is the target CF. It is no longer used as a branch node for the next split but is stored in Q. On the contrary, $v_{father} = 2v_{child}$. As a result, the concentration of a node must be a target CF in Q, and the v of each leaf node is $\frac{1}{2^h}$ by definition.

3.2.2 Example: Multi-Target Preparation

The splitting-droplet sharing algorithm can be extended to handle the sample preparation problem of multi-target CF, which was recently discussed in [11]. DMFBs should prepare a set of target CFs at the same time Each target CF is still constructed individually in the interpolated dilution phase. Nevertheless, leaf nodes are inserted into a single shared min-heap in the exponential dilution phase. In most cases, the unified min-heap can effectively reduce sample usage [11]. Our algorithm is very likely to reduce the total sample usage further. Besides, the total dilution operation count, the total buffer usage, and the total waste count can all be minimized further. Fig. 6b demonstrates a two-target example, where two target CFs are $\frac{608}{1024}$ and $\frac{96}{1024}$, respectively.

Reaching Fig. 5 with Fig. 6, it is found that compared with the most advanced REMIA [11], our algorithm has significantly improved the reduction of samples and waste. However, the *ST* method proposed performs very well in sample minimization but worst in operation count, producing more waste than REMIA [11] in single-target preparation. More specifically, Algorithm 1 consumes 50% and 67% fewer samples than REMIA [11] in the above cases, respectively. Though the proposed algorithm is primarily designed for reactant and waste minimization, it still outperforms 40%.

4 Splitting Droplet Sharing Algorithm

The proposed splitting droplet sharing algorithm begins with the ratio decomposition stage and continues with the splitting graph construction stage and the waste droplet sharing stage.

4.1 Dilution Gradient Profile

Assuming droplets with intermediate CFs of each Q of target CF are available, one can only prepare target CFs by diluting the original sample (100%) with buffer (0%). Dilution concentration ranges its accuracy h=10; in other words, the concentrations of the sample and buffer can be expressed

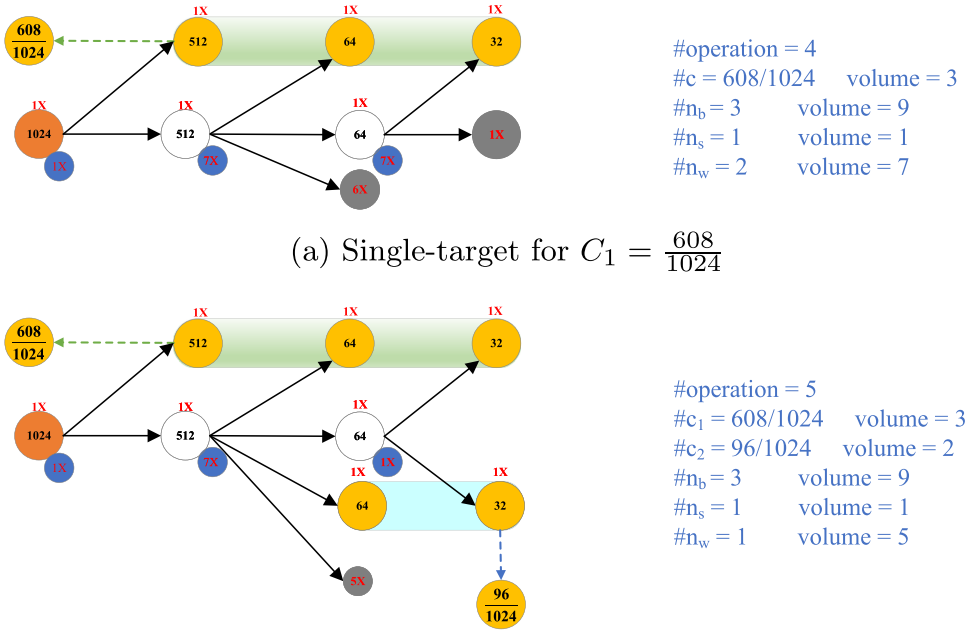

Fig. 6 Algorithm 1 for target CFs in Fig. 5

as $\frac{2^h}{2^h}$ and $\frac{0}{2^h}$. Afterward, some underlying combinatorial properties of the CFs are utilized favorably for producing a sequence of CFs by linearly adding exponents-CFs, which is represented as $\{\frac{2^h}{2^h}, \frac{2^{h-1}}{2^h}, \cdots, \frac{1}{2^h}, \frac{0}{2^h}\}$, where the elements are in geometric progression, can be quickly produced from the raw sample of CF $= \frac{2^h}{2^h}$ by serially mixing it with the buffer solution of CF $= \frac{0}{2^h}$. According to the relationship between target concentration C and dilution accuracy h in Formula 1, the range of target CFs C values is $[\frac{0}{1024}, \frac{1024}{1024}]$.

4.2 Proposed Algorithm

The algebraic expression for the composition of Q from $T_i \in T$ is described below.

$$Q = q_B 2^B + ... + q_b 2^b + ... + q_0 2^0 \tag{9}$$

Where $b \in B$ is the bits of the binary representation, the algorithm begins with the processing of input data, and the target CF is dissolved into leaf nodes (lines 1-3). This step transforms the given T_i into a polynomial representation Q_i. The set Q is constructed by including expressions Q_i as its elements (line 4). Empty set ST_i is created for T_i in the ratio decomposition stage (line 5). The ratio decomposition stage is formed to count the ratio of K droplets of each ST_i after selecting the minimum concentration of droplet K (line 6). The ratio decomposition stage determines an optimal concentration ratio (RST), depending on the minimum available concentration K. The splitting graph construction stage builds GST according to RST (line 7), where $< node >$ of ST_i are created and added.

Algorithm 2 Droplet-Sharing Dilution Algorithm

Require: n, T
Ensure: n_s, n_w, GST
1: **while** $T_i \in T$ **do**
2: Form algebraic expression Q_i for T_i
3: **end while**
4: Form set $Q = \{Q_1, Q_2, ..., Q_n\}$
5: Create empty sets $ST_i, i = 1, 2, ...$
6: $RST \Leftarrow$ Ratio decomposition stage
7: $GST \Leftarrow$ Splitting graph construction stage
8: $CP \Leftarrow$ Waste droplet recycling stage

Example:
There is an example with the following target CFs C.

1. Types of required different concentrations $n = 7$.
2. The precision level of concentration representation $h = 10$.
3. A Set of exponential gradient ratios of target CF T.

   $T = \{64, 160, 208, 232, 244, 248, 252\}$.

4. A set of target CF C of n types of required different concentrations ($n = 7, h = 10$).

   $C = \{\frac{64}{2^{10}}, \frac{160}{2^{10}}, \frac{208}{2^{10}}, \frac{232}{2^{10}}, \frac{244}{2^{10}}, \frac{248}{2^{10}}, \frac{252}{2^{10}}\}$

During processing (Fig. 8b), $Q_i (i = 1, ..., n)$ is analyzed according to Eq. 9. As a result, algebraic expressions $Q_i (i = 1, ..., n)$ for target CF $T_i (i = 1, ..., n)$ are formed, where

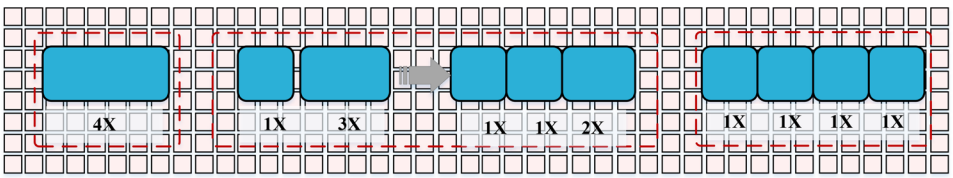

Fig. 7 Splitting model on MEDAs. MEDA biochip enabled splitting ratios which supports (1:3), (1:1:2), and (1:1:1:1)

$n = 7$. The element $node = \langle s, v \rangle$ in Q represents the leaf nodes with a concentration of v, and there is s in ST. The splitting graph GST builds the set of minimum STs that represents Q to achieve the given target CF (C) (Fig. 8c). Therefore, $Q = \{< 6, \frac{128}{1024} >, < 6, \frac{64}{1024} >, < 5, \frac{32}{1024} >, < 4, \frac{16}{1024} >, < 3, \frac{8}{1024} >, < 2, \frac{4}{1024} >\}$.The concentration of the direct product droplets generated by mixing the reagent droplets of concentration one and the buffer droplets is set to K. As shown in Fig. 8d, $K = \frac{128}{1024}$ and ST_i in GST have the reagents of concentration 1 to generate droplets of concentration $\frac{128}{1024}$ in the range of 1-8. According to Algorithm 1, six $\frac{128}{1024}$ droplets must be developed in ST_1, and $node_1$ is $< 6, \frac{128}{1024} >$ into queue Q. In addition to this, two $\frac{128}{1024}$ droplets in ST_1 generate four $\frac{64}{1024}$ droplets.

4.3 Ratio Decomposition Stage

The ratio decomposition stage determines quantity sequence RST, which stores the number of node $count$ with a concentration K for all STs.

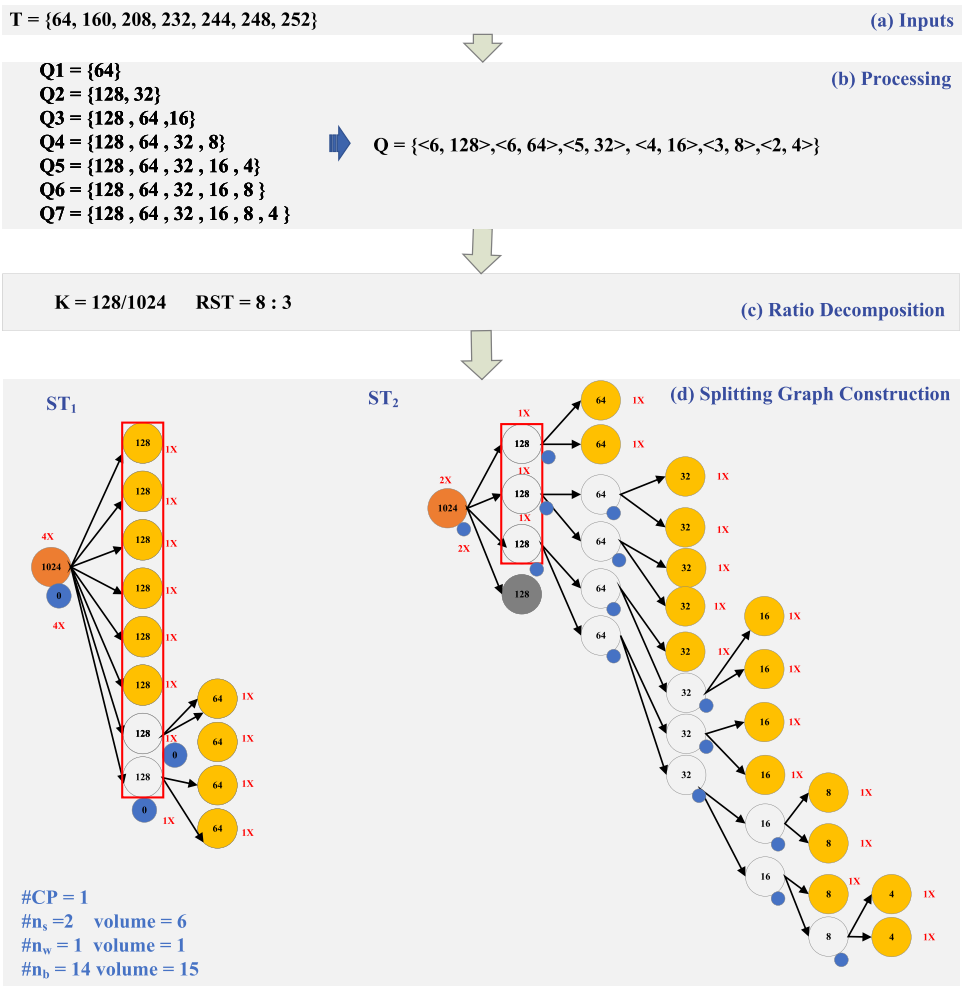

Fig. 8 Example demonstrating the splitting-droplet sharing algorithm. (a) Inputs: $T = \{64, 160, 208, 232, 244, 248, 252\}$ (b) Processing. (c) Ratio decomposition. (d) Splitting graph construction

Algorithm 3 Droplet-Sharing Dilution Algorithm

```
Require: K, Q
Ensure: RST, GST
1: h_K ⇐ log_2^{1/K}
2: count ⇐ 0
3: j ⇐ 2^{h_K − 1}
4: if Q ≠ ∅ ∩ v_j == K then
5:     count + +
6:     j + +
7: else
8:     RST.push(count)
9: end if
```

The algorithm uses $node =< s, v >$ to record the number of droplets with the same product concentration in the T_i ($T_i \leq 1$) to improve droplet utilization When T_i can generate nodes of the same attention, the split tree of Algorithm 1 can create nodes in bulk. It can also be seen from Fig. 6 that when the MEDA biochip is undergoing multi-sample preparation, the generation of droplets of target cf generates waste droplets (w). The waste droplets w are not recycled but go into a specific area of the chip waiting to be reactivated, a process we call the waste droplet sharing stage. Queue Q in Algorithm 2 stores the generated nodes; as shown in Algorithm 2, the initial element of Q is source CF, where source CF equals one or w. w is the waste generated from the initial biochemical reaction of the MEDA biochip using reagent droplets with a concentration of 1, which does not increase the sample dosage. Moreover, the volume of product droplets generated by MEDA biochip dispensing does not exceed eight times the minimum volume, so the minimum book of both source and w is $\frac{1}{8}$ times the reagent concentration.

In Algorithm 1, w is to prove to be the minimum available waste with concentration K. For example, Fig. 8c shows $w = \{\frac{128}{1024}, \frac{256}{1024}\}$. $\frac{256}{1024}$ is not the target CF. The result of ST_1 is eight $\frac{128}{1024}$, of which six are the direct targets and the other two splits, resulting in 4 $\frac{64}{1024}$. In addition, all target CF in the ST_2 may be generated by three $\frac{128}{1024}$. As depicted in Fig. 8d minimum wastage concentration $K = \frac{128}{1024}$.

The step of Algorithm 3 is to work out *RST*, which consists of the ratio of the number of *nodes* in each *ST* with the same concentration K. For example, in the example of Fig. 8, there are eight nodes with $\frac{128}{1024}$ in ST_1 and at least three $\frac{128}{1024}$ respectively in ST_2. ST_2 is three instead of four primarily because the *ST* generates nodes from top to bottom, and nodes of $\frac{256}{1024}$ generates two $\frac{128}{1024}$ at a time. However, according to one $\frac{128}{1024}$ is useless and stored as waste. Therefore, as shown in Fig. 8d, the *RST* of *GST* is 8:3.

4.4 Splitting Graph Construction Stage

The construction process of ST_1 in the example shown in Fig. 8 is shown in Fig. 9. The main idea of this stage is to construct an *ST* for each target CF and then combine them

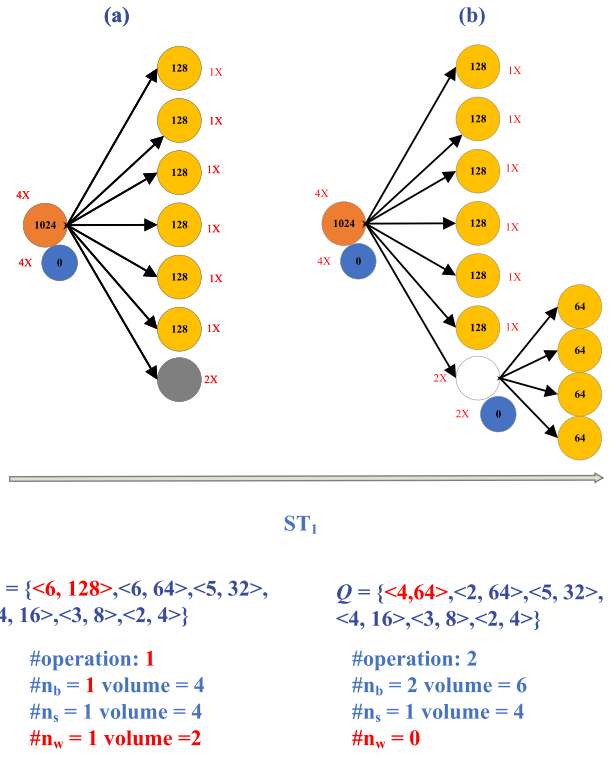

Fig. 9 Construction of ST_1 for the example in Fig. 8

to obtain the resultant splitting graph *GST*. This stage begins with constructing ST_i for the target CF set Q. First, subgraphs are built for elements $\langle s, v\rangle$ in the target set Q (line 3), as shown in Fig. 9. As shown in Fig. 9a dequeue element $\langle 6, \frac{128}{1024}\rangle$ from Q, which infers from the concentration $\frac{128}{1024}$ that it is in the third layer of *ST*, and the maximum number of nodes is eight. Figure 9b shows that eight $\frac{128}{1024}$ nodes are generated. The other two are used as the intermediate nodes of the *ST*. As shown in Fig. 9c, the head element of squadron Q is $\langle 6, \frac{64}{1024}\rangle$. Since two nodes with a concentration $\frac{128}{1024}$ generate four $\frac{64}{1024}$, there is no intermediate node to be split in the *ST*. Instead, the element$\langle 2, \frac{64}{1024}\rangle$ is modified, as shown in Fig. 9c. When the *drop* is false, and *STs* are returned. Therefore, in the *ST*, *drop* must be judged when mapping the elements in Q. When *drop* is false, it indicates that the leaf nodes are nodes with target CF. An *ST* is currently established to generate the element concentration in Q.

In general, *GST* represents the sequence of splitting droplets to produce droplets of all the target CF, starting from splitting level 0 with the input reagents and progressing upward with the next splitting level until the target CF is reached. Subgraphs whose lowest nodes are at the same level are combined to create nodes for the upper level, and this combining process will continue until it turns out to be a full binary tree. At this time, observe the leaf nodes of this tree, and the number exceeds $\langle s_i, v_i\rangle$ indicated drop is split

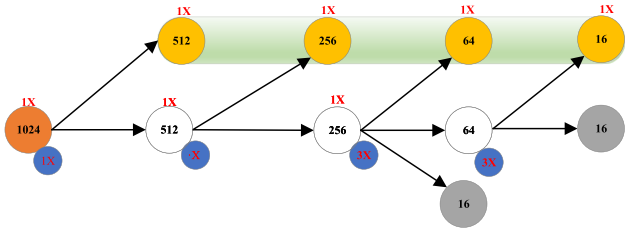

Fig. 10 Construction of example with target CF $= \frac{848}{1024}$

down one layer to generate $\langle s_{i+1}, v_{i+1} \rangle$. And then, the graphs ST_i are combined to construct the resultant splitting graph $GST = \{ST_1, ST_2, ..., ST_n\}$, such that

$$GST = ST_1 \bigcup ST_2 \bigcup ... \bigcup ST_n \tag{10}$$

Example:

Based on the channel dispensing shown in Fig. 2, the splitting model on MEDA biochips has been elaborated, which refers to the process of k 1X droplets formed through $k-1$ channel dispensing, represented as (1:1:1:1), as Fig. 7 shown. Moreover, a a general class of exponential gradients can be generated, successfully mixing the intermediate droplet closest to the target droplet concentration with the buffer solution. Let us briefly revisit the method of scanning the h-bit binary representation of the numerator of a desired CF. The following example illustrates the generation of target CF $= \frac{848}{1024}$ starting from sample (CF $= \frac{1024}{1024}$) and buffer (CF $= \frac{0}{1024}$), i.e., for $h = 10$. The 10-bit binary representation of the numerator of $\frac{848}{1024}$ is (1101010000). Convert the scanned "1" to a corresponding exponential representation while scanning the bits in its binary representation from right to left and outputs the required exponential-CFs: $\{\frac{512}{1024}, \frac{256}{1024}, \frac{64}{1024}, \frac{32}{1024}$ in array variable. As shown in Fig. 10, using a droplet with an initial concentration of 100% (CF $= \frac{1024}{1024}$), four exponential droplets can be generated through four split operations as described above. Every splitting step in the splitting droplet sharing algorithm must have produced one CF-value halved over that of the previous gradient. Finally, mix up all the exponential representations obtained from "1" from left to right to generating a particular target-CF. The number of waste liquid droplets generated was reduced by developing the target concentration to two. More importantly, the number of sample droplets was one, and four splitting and one mixing operation were used.

Table 4 Experiment setup

Test	T
Test 1	64, 160, 208, 232, 244, 250, 253
Test 2	512, 320, 224, 176, 152, 140, 134, 131
Test 3	256, 640, 832, 928, 976, 1000, 1012, 1018, 1021
Test 4	1024, 768, 640, 576, 544, 528, 520, 516, 514, 513
Test 5	128, 192, 224, 240, 248, 252, 254, 255

Target-CF is $C = T/1024$

4.5 Algorithm Complexity

An ST is a complete binary search tree having $2^h - 1$ nodes, where each node represents a CF-value in the target set T. The nodes labeled with CF $= \{\frac{2^h}{2^h}, \frac{2^{h-1}}{2^h}, \cdots, \frac{1}{2^h}, \frac{0}{2^h}\}$ appear as leaf nodes of ST, and the source droplets (CF $= \frac{2^h}{2^h}$) of ST appears as the root of ST. Also, the target CF can be expressed as a mixture of intermediate droplets, so the time complexity of ST is the time complexity of finding non-leaf nodes represented as intermediate concentrations, i.e., $O(N \log_2 N)$. The Time complexity of Algorithms 2 and 3

Table 3 Average sample/waste/operation count in single-target preparation

	$\#n_s$		$\#n_w$		#operation	
T	REMIA [3]	Proposed	REMIA [3]	Proposed	REMIA [3]	Proposed
2	5	1	8	9	14	9
4	5	1	8	8	14	8
8	5	1	8	7	14	7
16	5	1	8	6	14	6
32	5	1	8	5	14	5
64	5	1	8	4	14	4
128	9	1	8	3	18	3
256	11	1	10	2	22	2
512	11	1	10	1	22	1
1023	13	1	12	1	26	7
Average	10.05	1.00	10.32	4.16	21.37	4.79

Target-CF is $C = T/1024$

Table 5 Average sample/waste count in multi-target preparation

Range of		$\#n_w$ (%)			$\#n_s$ (%)		
Target-CFs	n	Proposed	REMIA [3]	EDT [2]	Proposed	REMIA [3]	EDT [2]
(64, 256)	7	1	66.67%	66.67%	1.508	24.80%	50.80%
(128, 512)	8	0	-0.06%	100%	1.750	12.50%	12.50%
(128,1024)	8	1	28.69%	50%	2.250	29.00%	-12.50%
(256, 1024)	10	0	34.31%	100%	7.504	16.62%	24.80%
(512,1024)	10	0	52.19%	100%	5.999	14.29%	14.30%

Number of different target CF in C is n

Gradient concentration range its accuracy h=10

Target CFs of the target set corresponding to Test in Table 4 is Range of Target-CFs

is the same, $O(N)$). Therefore, the algorithm proposed has a $O(N)$ complexity.

5 Simulation Results

5.1 Single-Target Preparation

To measure the performance of the splitting graph stage, we have conducted a single-target preparation experiment on the statistics of sample/waste/operation count in the concentration range of $C \in [\frac{1}{1024}, \frac{1023}{1024}]$. To demonstrate the effectiveness of *ST* in the splitting graph stage, we compare it against the sample mentioned earlier, REMIA [3]. Table 3 gives the partial experimental results. The averages over 1023 different concentration settings are reported. The results indicate that *ST* performs very well in sample minimization and operation count but produces more waste for single-target preparation. More specifically, *ST* consumes 90.04% less sample, 59.69% less waste droplet, and 77.59% less operation amount as compared with REMIA [3]. The results demonstrate that minimizing valuable reactants instead of waste can achieve a better outcome. In fact, after examining all 1023 cases, *ST* always wins or ties in sample usage for every patient compared with REMIA [3]. Table 3 also enumerates some extreme cases in which *ST* significantly improves. The sample usage can be decreased up to 90.91% for concentration $\frac{512}{1024}$, besides the waste droplet and operation count all have been cut down to 1, compared with REMIA [3], the results are 10 and 22. Most surprisingly, *ST* even outperforms the best in waste amount for some cases. For example, when the concentration is $\frac{512}{1024}$ and $\frac{1023}{1024}$, the amount of waste count is reduced to 1, 90% and 91.67% respectively.

5.2 Multi-Target Preparation

To evaluate the effect of the waste droplet recycling stage proposed in this paper on reducing samples and waste, we have detailedly analyzed the implementation process of EDT [2]. The multi-target preparation experiment on the statistics of sample and waste is in Table 4 [2], and the results are shown in Table 5.

Table 5 showing The sample usage of five tests presents the same set of data as in Table 4. When $n = 7$, the average amount of sample drops is about 1.5; when $n = 8$, the average value is 2.25; in an extreme case, $n = 10$, the amount of sample drops is 6. In these three cases, our algorithm improves the sample saving rate of 25%, 12.5%, and 14.29%, respectively. Overall, compared with REMIA [3], the proposed algorithm reduces $\#n_s$ by 24.80%, 12.50%, 16.62%, 14.29% and 0.29% respectively.

Table 5 also illustrates this conclusion concerning waste-saving. Moreover, the average reduction of reactant usage is 10.84% as Table 5 demonstrated. The removal of waste usage is up to 66.7%, which should be considered notable since the proposed algorithm does not pay extra attention to minimizing the operation count. More significantly, the waste amount is reduced to 0 in test2, test4, and test5, as shown in Table 5, concluding that the splitting-droplet sharing algorithm is the most effective waste minimization.

6 Conclusion and Future Work

Sample preparation is a fundamental process in biochemical reactions. Several techniques have been proposed to address this issue in the past few years, while only some focus on the multiple preparation gradient dilution samples. In this paper, we proposed a new splitting-droplet sharing algorithm for both reactant and waste minimization in multiple preparation gradient dilutions. It then successfully applies droplet sharing and waste droplet recycling to reduce the waste further using concurrence preparation of the same target. The experimental results demonstrated that all three phases of the splitting-droplet sharing algorithm have their contributions during optimization. The results also showed that the splitting-droplet sharing algorithm outperforms the existing state-of-the-art algorithm REMIA [11] and EDT [2] in terms of waste

amount and sample usage for exponential gradient dilution preparation. Lastly, the splitting-droplet sharing algorithm is also very efficient when the number of target sets increases. Consequently, it is concluded that the splitting-droplet sharing algorithm is a better alternative for multi-target sample preparation on digital microfluidic biochips. This article aims to consider the error analysis caused by droplet splitting and the chip area used for mixing operations in the proposed sample preparation algorithm in future research. At the same time, considering that MEDA biochips have the characteristic of real-time sensing of droplets, it is also necessary to upgrade and modify the sample preparation algorithm as needed to meet more common practical needs.

Acknowledgements This work was supported by the fund of Fujian Province Digital Economy Alliance, the National Natural Science Foundation of China (No. U1905211), and the Natural Science Foundation of Fujian Province (No.2020J01500).

Data Availibility The datasets generated and analyzed during The current study is available from the corresponding author upon reasonable request.

Declarations

Conflict of Interest The authors declare that they have no known competing financial interests or personal relationships that could have appeared to influence the work reported in this paper.

References

1. Bhattacharjee S, Banerjee A, Ho TY et al (2013) On producing linear dilution gradient of a sample with a digital microfluidic biochip. IEEE Comput Soc USA 5:77–81. https://doi.org/10.1109/ISED.2013.22
2. Bhattacharjee S, Banerjee A, Ho TY et al (2019) Efficient generation of dilution gradients with digital microfluidic biochips. IEEE Trans Comput Aided Des Integr Circuits Syst 38(5):874–887. https://doi.org/10.1109/TCAD.2018.2834413
3. Bhattacharjee S, Poddar S, Roy S et al (2016) Dilution and mixing algorithms for flow-based microfluidic biochips. IEEE Trans Comput Aided Des Integr Circuits Syst 36(4):614–627. https://doi.org/10.1109/TCAD.2016.2597225
4. Dong C, Liu L, Liu H et al (2020) A survey of dmfbs security: State-of-the-art attack and defense. In: 2020 21st International Symposium on Quality Electronic Design (ISQED), p 14–20. https://doi.org/10.1109/ISQED48828.2020.9137016
5. Friedrich D, Please CP, Melvin T (2012) Design of novel microfluidic concentration gradient generators suitable for linear and exponential concentration ranges. Chem Eng J 193–194:296–303. https://doi.org/10.1016/j.cej.2012.04.041
6. Guo W, Lian S, Dong C et al (2022) A survey on security of digital microfluidic biochips: Technology, attack, and defense. ACM Trans Des Autom Electron Syst 27(4):33. https://doi.org/10.1145/3494697
7. Huang X, Liang CC, Li J et al (2019) Open-source incubation ecosystem for digital microfluidics – status and roadmap: Invited paper. In: 2019 IEEE/ACM International Conference on Computer-Aided Design (ICCAD), p 1–6. https://doi.org/10.1109/ICCAD45719.2019.8942172
8. Huang HC, Liang CC, Wang Q et al (2022) Nr-router: Non-regular electrode routing with optimal pin selection for electrowetting-on-dielectric chips. In: 2022 27th Asia and South Pacific Design Automation Conference (ASP-DAC), p 56–61. https://doi.org/10.1109/ASP-DAC52403.2022.9712567
9. Huang JD, Liu CH, Chiang TW (2012) Reactant minimization during sample preparation on digital microfluidic biochips using skewed mixing trees. In: Proceedings of the International Conference on Computer-Aided Design. Association for Computing Machinery, New York, NY, USA, 7, p 377–383. https://doi.org/10.1145/2429384.2429464
10. Huang JD, Liu CH, Lin HS (2013) Reactant and waste minimization in multitarget sample preparation on digital microfluidic biochips. IEEE Trans Comput Aided Des Integr Circuits Syst 32(10):1484–1494. https://doi.org/10.1109/TCAD.2013.2263035
11. Huang, Juinn-Dar, Liu et al (2015) Reactant minimization in sample preparation on digital microfluidic biochips. p 1429–1440. https://doi.org/10.1109/TCAD.2015.2418286
12. Hsieh YL, Ho TY, Chakrabarty K (2014) Biochip synthesis and dynamic error recovery for sample preparation using digital microfluidics. IEEE Trans Comput Aided Des Integr Circuits Syst 33(2):183–196. https://doi.org/10.1109/TCAD.2013.2284010
13. Jebrail MJ, Wheeler AR (2009) Digital microfluidic method for protein extraction by precipitation. Anal Chem 81(1):330–335. https://doi.org/10.1021/ac8021554
14. Lee CY, Chang CL, Wang YN et al (2011) Microfluidic mixing: A review. Int J Mol Sci 12(5):3263–3287. https://doi.org/10.3390/ijms12053263
15. Li Z, Chakrabarty K, Ho TY et al (2019) Micro-Electrode-Dot-Array Digital Microfluidic Biochips: Design Automation, Optimization, and Test Techniques. Design Automation, Optimization, and Test Techniques, Micro-Electrode-Dot-Array Digital Microfluidic Biochips
16. Li Z, Lai KYT, Chakrabarty K et al (2017) Droplet size-aware and error-correcting sample preparation using micro-electrode-dot-array digital microfluidic biochips. IEEE Trans Biomed Circuits Syst 11(6):1380–1391
17. Li Z, Lai YT, Chakrabarty K et al (2017) Droplet size-aware and error-correcting sample preparation using micro-electrode-dot-array digital microfluidic biochips. IEEE Trans Biomed Circuits Syst PP(99):1–12
18. Li Z, Lai KYT, Yu PH et al (2016) High-level synthesis for micro-electrode-dot-array digital microfluidic biochips. In: Proceedings of the 53rd Annual Design Automation Conference. Association for Computing Machinery, New York, NY, USA, 146, p 6. https://doi.org/10.1145/2897937.2898028
19. Liang TC, Chan YS, Ho TY et al (2019) Sample preparation for multiple-reactant bioassays on micro-electrode-dot-array biochips. In: Proceedings of the 24th Asia and South Pacific Design Automation Conference. Association for Computing Machinery, New York, NY, USA, 6, p 468–473. https://doi.org/10.1145/3287624.3287708
20. Liang TC, Chan YS, Ho TY et al (2020) Multitarget sample preparation using meda biochips. IEEE Trans Comput Aided Des Integr Circuits Syst 39(10):2682–2695. https://doi.org/10.1109/TCAD.2019.2942002
21. Mitra D, Roy S, Bhattacharjee S et al (2014) On-chip sample preparation for multiple targets using digital microfluidics. IEEE Trans Comput Aided Des Integr Circuits Syst 33(8):1131–1144. https://doi.org/10.1109/TCAD.2014.2323200
22. O'Neill AT, Monteiro-Riviere N, Walker GM (2006) A serial dilution microfluidic device for cytotoxicity assays. In: 2006 International Conference of the IEEE Engineering in Medicine and Biology Society. IEEE, New York, NY, USA, p 2836–2839. https://doi.org/10.1109/IEMBS.2006.259270
23. Ottesen EA, Hong JW, Quake SR et al (2006) Microfluidic digital PCR enables multigene analysis of individual environmental

bacteria. Lab on a Chip 314(5804):1464–1467. https://doi.org/10.1126/science.1131370
24. Poddar S, Bhattarcharjee S, Nandy SC et al (2018) Optimization of multi-target sample preparation on-demand with digital microfluidic biochips. IEEE Trans Comput Aided Des Integr Circuits Syst, p 1–1
25. Quan PL, Sauzade M, Brouzes E (2018) dpcr: a technology review. Sensors 18(4):1271. https://doi.org/10.3390/s18041271
26. Ren H, Srinivasan V, Fair RB (2003) Design and testing of an interpolating mixing architecture for electrowetting-based droplet-on-chip chemical dilution. In: TRANSDUCERS'03. 12th International Conference on Solid-State Sensors, Actuators and Microsystems. Digest of Technical Papers (Cat. No. 03TH8664), p 619–622. https://doi.org/10.1109/SENSOR.2003.1215549
27. Roy S, Bhattacharya BB, Chakrabarty K (2010) Optimization of dilution and mixing of biochemical samples using digital microfluidic biochips. IEEE Trans Comput Aided Des Integr Circuits Syst 29(11):1696–1708
28. Roy S, Bhattacharya BB, Chakrabarty K (2011) Waste-aware dilution and mixing of biochemical samples with digital microfluidic biochips. In: 2011 Design, Automation & Test in Europe. IEEE, Grenoble, France, p 1–6. https://doi.org/10.1109/DATE.2011.5763174
29. Saiki RK, Gelfand DH, Stoffel S et al (1988) Primer-directed enzymatic amplification of DNA with a thermostable. DNA polymerase 239(4839):487–491
30. Sun M, Bithi SS, Vanapalli SA (2011) Microfluidic static droplet arrays with tuneable gradients in material composition. Lab on a Chip 11(23):3949–3952. https://doi.org/10.1039/c1lc20709a
31. Thies W, Urbanski JP, Amarasinghe TS (2008) Abstraction layers for scalable microfluidic biocomputing. Nat Comput 7(2):255–275. https://doi.org/10.1007/s11047-006-9032-6
32. Walker GM, Monteiro-Riviere N, Rouse J et al (2007) A linear dilution microfluidic device for cytotoxicity assays. Lab on A Chip 7(2):226–232. https://doi.org/10.1039/B608990A
33. Wang J, Brisk P, Grover WH (2016) Random design of microfluidics. Lab on A Chip 16(21):4212–4219. https://doi.org/10.1039/C6LC00758A
34. Zhang L, Li Z, Huang X et al (2023) Enhanced built-in self-diagnosis and self-repair techniques for daisy-chain design in meda digital microfluidic biochips. IEEE Trans Comput Aided Des Integr Circuits Syst 42(10):3236–3249. https://doi.org/10.1109/TCAD.2023.3244524
35. Zhong Q, Bhattacharya S, Kotsopoulos S et al (2011) Multiplex digital PCR: breaking the one target per color barrier of quantitative. PCR 11(13):2167. https://doi.org/10.1039/c1lc20126c

Dong Chen received the B.S. and M.S. degrees in computer science, Fuzhou University, China, in 2002 and 2005 respectively, and the Ph.D. degree in computer science from the Computer School, Wuhan University, China, in 2011. She was a visiting researcher with the University of California at Los Angeles (UCLA), from 2015 to 2016. She is currently an Assistant Professor with the College of Computer and Data Science, Fuzhou University. Her research interests include intelligent computing, and IC physical and security design.

Xiao Chen received the B.S. degrees in vehicle engineering from the college of Mechanical and Electrical Engineering of Xi'an University of Architecture and Technology, China, in 2019, and the M.S. degree with the College of Computer and Data Science of Fuzhou University, China, in 2023, respectively. Her research interests include biochip privacy protection, data security, differential privacy, chip security.

Zhenyi Chen received the B.S. and M.S. degrees in computer science from the College of Computer and Data Science, Fuzhou University, China, in 2000 and 2005, respectively, and the Ph.D. degree in computer science from the Computer School, Wuhan University, China, in 2012. He is currently pursuing the second Ph.D. degree with the Department of Computer Science and Engineering, University of South Florida. His research interests include swarm intelligence, optimization, database and smart manufacturing.